PHYSICAL REVIEW C

NUCLEAR PHYSICS

THIRD SERIES, VOLUME 26, NUMBER 3 SEPTEMBER 1982

Photoneutron cross sections for ^{15}N

J. W. Jury,* B. L. Berman, and J. G. Woodworth
Lawrence Livermore National Laboratory, University of California, Livermore, California 94550

M. N. Thompson
School of Physics, University of Melbourne, Parkville, Victoria 3052, Australia

R. E. Pywell
Accelerator Laboratory, University of Saskatchewan, Saskatoon, Saskatchewan S7N 0W0, Canada

K. G. McNeill
Department of Physics, University of Toronto, Toronto, Ontario M5S 1A7, Canada
(Received 29 December 1981)

Photoneutron cross sections involving the emission of one and two neutrons from ^{15}N have been measured over the excitation energy interval from threshold (10.8 MeV) to 38 MeV using monoenergetic photons from the annihilation in flight of fast positrons. A very broad giant dipole resonance extending from about 16 to 30 MeV was observed, with a maximum (γ,n_{tot}) cross section of about 11 mb at 23.5 MeV. The magnitude of the measured average photoneutron energies shows that most of the strength below 15 MeV decays to the ground state of ^{14}N, whereas most of the strength in the giant resonance decays to excited states. Comparison with particle-capture cross-section data indicates that multiparticle-multihole interference effects probably account for some of the pronounced intermediate structure observed above 16 MeV in the (γ,n) cross section. Comparison with a recent shell-model calculation favors the use of a Tabakin potential over a δ-function force with a Soper exchange mixture, in marked contrast with recent corresponding results for ^{13}C and ^{17}O. Features of recently measured photoreaction cross sections for the ^{12}C, ^{13}C, ^{14}N, ^{15}N, ^{16}O, ^{17}O, and ^{18}O nuclei are compared as well.

NUCLEAR REACTIONS $^{15}N(\gamma,n)$, $E_\gamma=10.8-38.0$ MeV; measured 4π neutron yield for monoenergetic photons; $(E_\gamma,1n)$, $(E_\gamma,2n)$, integrated cross sections; comparisons of results with other reaction channels and with cross sections for neighboring nuclei; comparison with shell-model theory.

I. INTRODUCTION

Much of what we know about the nuclear reaction mechanisms for the giant dipole resonance (GDR) (see Refs. 1) has been learned from experimental and theoretical photonuclear studies of ^{12}C and ^{16}O, particularly the latter (see Refs. 2), because samples of these nuclei are readily available and easy to work with in the laboratory and because the structure of these nuclei is particularly simple to deal with theoretically. A logical extension of these studies of ^{12}C and ^{16}O is the study of their neighbors in the periodic table.

The nature of the photoreaction mechanism in the mass-15 nuclei has been the object of intensive investigation over the last decade. Many measurements, listed in Table I, have been carried out on the ^{15}N system (Refs. 3–20) in order to delineate

 ©1982 The American Physical Society

TABLE I. Photonuclear reactions on ^{15}N.

Reaction	Previous references	Threshold (MeV)
^{15}N(γ,p_0)	3, 4, 5	10.2
^{14}C(p,γ_0)	6, 7, 8, 9	
^{15}N(e,p_0)	10	
^{15}N(γ,n_0)	11	10.8
^{14}N(n,γ_0)	12	
^{15}N(γ,α_0)		11.0
^{11}B(α,γ_0)	13, 14	
^{15}N(γ,n_1)		13.1
^{15}N(γ,t_0)		14.8
^{12}C(t,γ_0)	15	
^{15}N(e,t_0)	16	
^{15}N(γ,d_0)	17	16.2
^{13}C(d,γ_0)	17, 18, 19	
^{15}N(γ,p_1)	5	16.3
^{15}N(γ,pn)		18.4
^{15}N($\gamma,2n$)		21.4
^{15}N($\gamma,\alpha n$)		22.4
^{15}N(e,e')	20	

the properties of various reaction channels. The threshold energies for these and other relevant photonuclear reaction channels for ^{15}N also are given in Table I.

Conspicuously absent from this list of reactions is the one which contains the major component of photoabsorption strength, the (γ,n_{tot}) reaction. This reaction can proceed via both the $T_< = T_0 = \frac{1}{2}$ and $T_> = T_0 + 1 = \frac{3}{2}$ components of the GDR and, when taken together with information on the uniquely $T_<$ (γ,n_0) channel, can provide a test of theories describing the distribution of isospin strength across the GDR. Limited availability of sufficient ^{15}N separated-isotope sample material might be the reason that this reaction has gone unmeasured until now: A measurement of the total photoneutron cross section typically requires molar quantities of sample material under present-day experimental conditions.

The measurement reported here constitutes part of a series of experiments on the light nuclei with one or two valence nucleons (or holes) associated with a core, such as ^{13}C, ^{17}O, and ^{18}O (Refs. 21–23, respectively), undertaken at the Lawrence Livermore National Laboratory. The sample used for this measurement consisted of a considerable quantity of gaseous separated-isotope ^{15}N, which was used in the new Livermore gaseous target facility.[24,25] This sample containment vessel was used with the existing 4π neutron detector and the positron-annihilation monoenergetic photon facility at the Livermore electron-positron linear accelerator. This combination facilitated the measurement of the (γ,n) and ($\gamma,2n$) cross sections for ^{15}N from threshold (10.8 MeV) to 38 MeV.

Much of the experimental work on ^{15}N has been carried out to study its specific reaction properties, because ^{15}N differs by only one proton-hole from the well-studied ^{16}O closed-shell nucleus. For the same reason, several theoretical descriptions of the cross section for photoabsorption of mass-15 nuclei have been formulated,[26,27] the most recent of which is the shell-model calculation of Albert *et al.*[28] for ^{15}N. The cross sections measured here can be used to test whether or not the shell-model calculation of Ref. 28 using a δ-function potential with a Soper mixture of exchange forces describes the 1p-2h GDR for this nucleus as well as it does those for the 2p-1h nuclei ^{13}C and ^{17}O (Ref. 29).

Finally, a measurement of the ^{15}N(γ,n_{tot}) cross section provides a valuable insight into the physics of the *p*-shell nuclear reactions because a detailed comparison of the photoneutron cross sections for ^{14}N (Ref. 30), ^{15}N, and ^{16}O (Refs. 31) is now possible. Analysis of this series can complement the current theories of valence-nucleon or valence-hole core polarization at mass 16 and of multiparticle-multihole residual interactions at this well-investigated nuclear mass number.

II. EXPERIMENTAL DETAILS

A complete description of the experimental facilities and procedures can be found in Ref. 23. The pressurized-gas sample container is described in detail in Ref. 25. Therefore, only a brief description of the apparatus and techniques is presented here.

A pulsed positron beam from the electron-positron linear accelerator, energy-selected with a momentum resolution of $\sim 1\%$, was incident upon a 0.76-mm thick beryllium annihilation target, producing both annihilation and bremsstrahlung radiation. Positrons passing through the annihilation target were swept by a magnet into a well-shielded

beam dump. Under these conditions, the energy resolution of the annihilation-radiation component of the photon beam varied from 150 keV (FWHM) for photon energies near 11 MeV to about 450 keV for the highest energies used.

The collimated photon beam passed through a calibrated transmission ion chamber and then through the high-pressure-gas photonuclear sample (see Fig. 1 of Ref. 24). Surrounding the tubular gas sample was the 4π neutron detector, consisting of a 0.61-m cube of paraffin containing 48 BF_3 tubes arranged in four concentric rings of 12 tubes each. Because of neutron moderation in the paraffin, the ratio of the counting rate for the outer ring to that for the inner ring (the ring ratio) provides a measure of the average neutron energy (and hence of the detector efficiency) for each data point.

The 62.0-g ^{15}N sample was in the form of ^{15}N gas of isotopic purity 98.9%, contained in the 1-m long, 2.54-cm diameter (volume = 0.507 l) sample holder at a pressure of 11.5 MPa (113.5 atm). The extended length of this sample meant that photoneutrons produced near the ends were detected with a lower efficiency than those emitted at the center of the sample. In an extensive series of measurements using gaseous ^{16}O as a standard and analyzed together with Monte Carlo computer simulations, Faul *et al.*[25] have determined [at all average neutron energies (or ring ratios)] the ratio of this gas-sample efficiency to the well-determined central-point-source efficiency previously used for experiments at the Livermore facility (see Fig. 2 of Ref. 25).

The data-collection procedure involved the sequential measurement of sample-in data using both positrons and electrons (to enable subtraction of the photoneutrons produced by the positron bremsstrahlung) and sample-out (evacuated sample-holder) data [to enable the subtraction of photoneutrons produced in the windows and walls of the pressure vessel (and elsewhere)]. This background from the empty sample container was seen to be a small fraction ($\sim$20% in the GDR) of the counting rate for the container-plus-gas runs. Also, at alternate energy points, the measurements were repeated with the annihilation target removed to ascertain the counting rate for background events from cosmic rays, BF_3 tube noise, etc. This background counting rate was typically only one or two percent of the real-event counting rate for each data point.

III. DATA ANALYSIS

Details of the various steps in the data-reduction procedure to extract the $(\gamma,1n)$ and $(\gamma,2n)$ cross sections from the raw neutron-event data are described in Refs. 21–23; only a brief summary of the most important steps is presented here.

After the recorded neutron events were corrected for pileup in the detector (a correction of a few percent at most because of the low counting rates), the neutron backgrounds (annihilation target removed) were subtracted for both the positron and electron measurements. Because these backgrounds were very small, the uncertainty introduced by this procedure was negligible.

Because the energy spectrum of the annihilation-plus-bremsstrahlung radiation differs from that of purely bremsstrahlung photons, a measured correction was applied to the ion-chamber response to normalize the electron data to the positron data. The normalized electron data then were subtracted from the positron data, leaving the neutron counts which result only from the annihilation radiation.

The measured sample-blank (empty-pressure-vessel) data, normalized to equal photon flux, were subtracted from the vessel-full data to give the net ^{15}N results. After a small correction for the neutron multiplicity in each ring, the data were corrected for the energy-dependent efficiency of the neutron detector using the ring-ratio result for each energy.

The data then were converted to photoneutron cross sections by applying the measured ion-chamber response per photon (which was remeasured during 1979 and found to be consistent with the previous Livermore values), the known number of ^{15}N nuclei in the beam, and a small correction for the photon attenuation in the sample gas and the entrance windows.

IV. RESULTS

A. Cross sections

The photoneutron cross sections for ^{15}N measured in this experiment are shown in Fig. 1: Part (a) shows the total photoneutron cross section

$$\sigma(\gamma,n_{\text{tot}})=\sigma[(\gamma,n)+(\gamma,pn)+(\gamma,\alpha n)+(\gamma,2n)] ,$$

part (b) shows the single photoneutron cross section

$$\sigma(\gamma,1n)=\sigma[(\gamma,n)+(\gamma,pn)+(\gamma,\alpha n)] ,$$

and part (c) shows $\sigma(\gamma,2n)$. The plotted error flags represent the statistical uncertainties only. Possible systematic uncertainties which are associated with the cross sections do not exceed 7% at energies

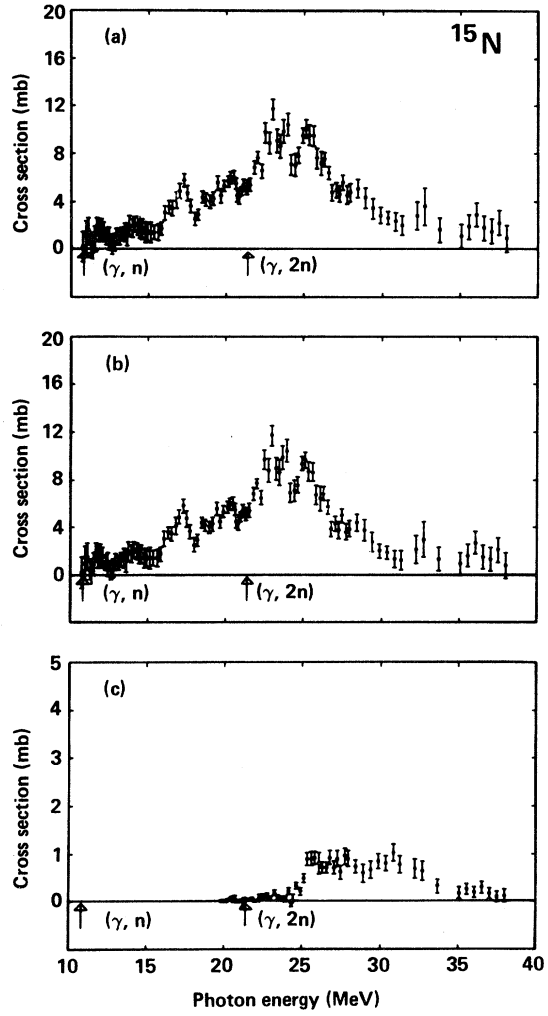

FIG. 1. Photoneutron cross sections for ^{15}N. Part (a) shows the total photoneutron cross section

$$\sigma(\gamma,n_{\text{tot}})=\sigma[(\gamma,n)+(\gamma,pn)+(\gamma,\alpha n)+(\gamma,2n)];$$

part (b) shows the single photoneutron cross section

$$\sigma(\gamma,ln)=\sigma[(\gamma,n)+(\gamma,pn)+(\gamma,\alpha n)];$$

part (c) shows $\sigma(\gamma,2n)$. The plotted error flags indicate the statistical uncertainties only. The threshold energies for the (γ,n) and $(\gamma,2n)$ reactions are indicated by arrows. Other photoreaction threshold energies are given in Table I.

below about 15 MeV but might reach as much as 20% at the higher energies measured.

Inspection of the (γ,n_{tot}) cross section in Fig. 1(a) shows the GDR to be centered near 23.5 MeV with a maximum value of about 11 mb, and to span the wide energy region from about 16 to 30 MeV. Considerable intermediate structure is observed in the GDR for this nucleus. In the region below about 16 MeV, an interpretation of the structure can be made which assumes that the photoneutron cross section will reflect the relatively simple single-particle excitations involved in decays to the ground state of ^{14}N. Evidence discussed below shows that even though transitions are kinematically possible to the $T=1$, 2.3-MeV first excited state in ^{14}N, nearly all the neutron decay strength from nuclear excitation below about 15 MeV proceeds via the (γ,n_0) channel. There is clear evidence in this low-energy region for a peak at 11.1 MeV and for additional structure centered at 11.8 and 14.1 MeV.

B. Average neutron energies

As discussed above, the configuration of the rings of BF_3 tubes in the detector allows a determination of the average energy of the emitted photoneutrons by taking the ratio of counts in the outer and inner rings. Figure 2 shows the results for the present measurements. It is interesting to note that the measured average neutron energy is very close to that expected for purely ground-state neutrons for excitation energies up to about 15 MeV. This implies that nearly all transitions are proceeding to the $T=0$ ground state of ^{14}N even though decays to the $T=1$ first excited state become possible at an excitation energy of 13.1 MeV (Table I). Evidence from the (γ,n_0) measurement of Watson *et al.*[11] and from a (γ,γ') measurement of Patrick *et al.*[32] indicates that ground-state transitions dominate the neutron reaction mechanism at least up to 15 MeV, and further, that no transitions to the $T=1$ first excited state occur until above 18 MeV. The curve in Fig. 2 also displays a peaking of the average neutron ener-

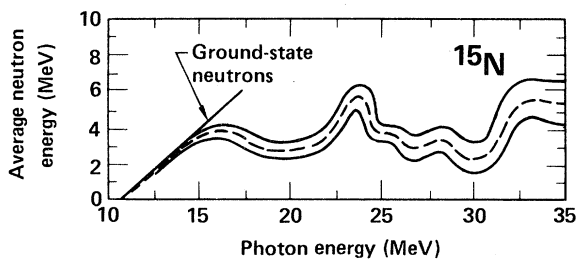

FIG. 2. The average energy of the emitted photoneutrons is plotted as a function of excitation energy in ^{15}N. These average energies were determined from the ring ratios. The light solid lines represent the statistical uncertainity associated with the ring-ratio measurement. The dark line represents the neutron energies expected if all transitions were to the ground state of ^{14}N.

gy near 23.5 MeV, the peak of the giant resonance. Perhaps at this energy the single-particle excitations from a ^{16}O-like configuration play the most significant role in the photoabsorption process, which might account for the observed rise of the average neutron energy here. This could be interpreted to signify that the proton hole in the ground-state configuration of ^{15}N has little effect upon the photoneutron reaction at the peak of the giant resonance. A comparison of the (γ,n) cross sections of ^{15}N and ^{16}O (see below) adds weight to this conjecture.

Finally, at energies near 33 MeV the average neutron energy once again is seen to rise significantly. This is an indication that there is a renewed onset of transitions to low-lying excited states in ^{14}N. The calculation of Albert *et al.*[28] using the Tabakin potential predicts substantial $T_< = \frac{1}{2}$ strength near this energy (see below). Although the evidence from the cross-section data [Fig. 1(a)] for a resonance near 33 MeV is weak, it might be the case that a resonance at this energy exists and decays to low-lying excited states of ^{14}N.

C. Integrated cross sections

The integrated photoneutron cross sections and their moments are given in Table II for the region from threshold to 38 MeV. The overall uncertainty associated with the $(\gamma,1n)$ integrated strength is no more than 10%. Since the Thomas-Reiche-Kuhn (TRK) sum-rule value for ^{15}N is $60NZ/A = 224$ MeV mb, it is seen that the fraction of the TRK sum rule exhausted by the photoneutron channels from threshold to 38 MeV is about 47% (105.9 MeV mb). It is interesting to note that the (γ,p_{tot}) measurement by Denisov *et al.*[5] results in an integrated strength of about 72 ± 10 MeV mb (from threshold to 30.5 MeV), while over the same energy interval the (γ,n_{tot}) integrated strength is 91 MeV mb. However, because the (γ,pn) threshold is 18.4 MeV (Table I), it is reasonable to assume that some single photoneutrons are accompanied by a

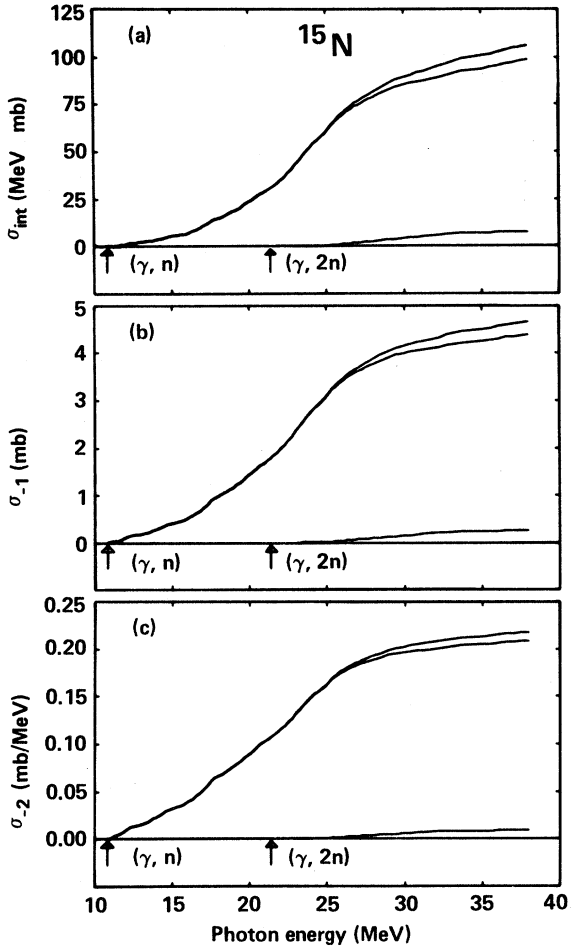

FIG. 3. Integrated photoneutron cross sections for ^{15}N are plotted as functions of the upper limit of integration. Part (a) shows the integrated cross sections $\sigma_{\text{int}} = \int \sigma(E_\gamma) dE_\gamma$ for the $(\gamma,2n)$ reaction (bottom curve), the $(\gamma,1n)$ reaction (middle curve), and their sum, the (γ,n_{tot}) reaction (top curve). Integrated cross sections over any desired limits can be obtained from these curves by subtraction. Parts (b) and (c) show the energy-weighted moments of the integrated cross sections

$$\sigma_{-1} = \int \sigma(E_\gamma) E_\gamma^{-1} dE_\gamma$$

and

$$\sigma_{-2} = \int \sigma(E_\gamma) E_\gamma^{-2} dE_\gamma ,$$

respectively.

TABLE II. Integrated cross sections for ^{15}N.[a]

Reaction	$\sigma_{\text{int}} = \int \sigma\, dE_\gamma$ (MeV mb)	$\sigma_{-1} = \int \sigma E_\gamma^{-1} dE_\gamma$ (mb)	$\sigma_{-2} = \int \sigma E_\gamma^{-2} dE_\gamma$ (mb MeV^{-1})
$(\gamma,1n)$	98.4	4.38	0.208
$(\gamma,2n)$	7.6	0.26	0.009
(γ,n_{tot})	105.9	4.63	0.216

[a]From threshold to 38.0 MeV.

proton, and thus the addition of the present cross section and the (γ,p_{tot}) data of Denisov might give an overestimate of the photoabsorption strength over this energy region.

The energy dependence of the integrated cross sections and their moments for ^{15}N are shown in Fig. 3, as running sums, in order to facilitate information retrieval. One also can see from this figure that the curves for σ_{-1} and σ_{-2} are flattening at the upper-energy limit of this measurement.

V. DISCUSSION

A. Comparison with other reaction channels

For clarity, the low-energy region of our measured $\sigma(\gamma,n_{tot})$ is shown with expanded scales in Fig. 4. Table III compares the energies of the peaks seen in this cross section with those seen in other reaction channels [(γ,n_0), (γ,p_0), (γ,d_0), (γ,t_0), (γ,α_0), and (e,e')]. In general, there is agreement of the present results with the peaks seen in the (γ,n_0), (γ,p_0), and (e,e') measurements. However, we note that the prominent *valleys* in the (γ,n) cross section at energies near 18, ~21, and 24.5 MeV appear to correlate with the *peaks* seen in the (γ,d_0) cross section (Refs. 17–19) at 17.7, 22, and 24 MeV. This correlation suggests that some of the intermediate structure in the ^{15}N giant resonance might arise from the same kind of two-particle

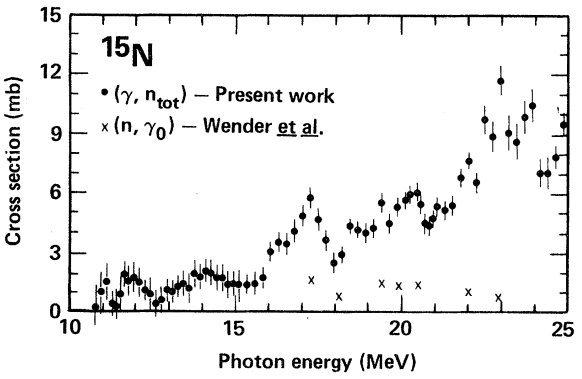

FIG. 4. The present total photoneutron cross section of Fig. 1(a) is shown with expanded scales and compared with the recent ground-state data of Wender *et al.*[12] This shows that $\sigma(\gamma,n_0)$ constitutes only a small part of $\sigma(\gamma,n_{tot})$ above ~17 MeV. [Only those points from Ref. 12 for which angular distributions were measured are plotted here; their 90° excitation function shows more detailed structure (see Table III).]

two-hole interference effects as is thought (Ref. 33) to be the case in the neighboring ^{16}O nucleus, where a similar pattern of intermediate structure appears.

Recently, Wender *et al.*[12] have made a measurement of the $^{14}N(n,\gamma_0)$ cross section as a function of laboratory angle over the excitation-energy region from 17.3 to 22.9 MeV in ^{15}N. Their results have been converted (by detailed balance) to cross sections for the $^{15}N(\gamma,n_0)$ reaction and also are shown in Fig. 4.

If all transitions were to proceed to the ground state of ^{14}N (as they do below about 15 MeV, as discussed in Sec. IV B above) the (γ,n_{tot}) and (γ,n_0) cross sections would be identical. It is clear from the figure, however, that by 17.3 MeV there is a significant difference between the two cross sections. Clearly, many non-ground-state transitions are taking place and the low average neutron energies for this region shown in Fig. 2 indicate that they are proceeding via highly excited states of ^{14}N. This is characteristic of the onset of a collective giant resonance. This can be contrasted with the case for ^{16}O (and ^{12}C) where most of the GDR decays via the ground-state channel (for both neutrons and protons). Therefore, it appears as if the presence of a proton hole in the ^{16}O core makes a significant change in the photoneutron reaction mechanism, altering the process from a relatively simple 1p-1h resonance-direct reaction in the ^{16}O core to a more complicated and perhaps slower process often resulting in the formation of highly excited ^{14}N.

B. Comparison with theory

The present results are compared with the recent theoretical calculation of Albert *et al.*[28] in Fig. 5, where the calculated $\sigma(\gamma,\text{tot})$ results were renormalized in order to facilitate visual comparison with the present $\sigma(\gamma,n_{tot})$ data. This calculation employs a two-hole one-particle shell model with either a zero-range Soper or a separable Tabakin residual interaction. The calculation assumes a closed ^{16}O core which is filled up to the $1p_{1/2}$ harmonic-oscillator state. Only $E1$ and $M2$ transitions to non-normal-parity states were considered. These states were constructed by using up to two holes in the single-particle states $1s_{1/2}$, $1p_{3/2}$, and $1p_{1/2}$ and up to one particle in the $1d_{5/2}$, $2s_{1/2}$, and $1d_{3/2}$ states. Using single-particle energies similar to those used in a previous calculation by Fraser *et al.*,[26] the zero-range Soper interaction and a separable Tabakin interaction were applied in the same manner as in similar calculations of the ^{13}C and ^{17}O

TABLE III. Peaks in the photonuclear cross sections for ^{15}N (in MeV).

(γ,n) This work	(n,γ_0) Ref. 12	(p,γ_0) Ref. 6	(γ,p_0) Ref. 3	(γ,p_0) Ref. 4	(γ,p_0) Ref. 5	(e,p_0) Ref. 10	(p,γ_0) Ref. 7	(p,γ_0) Ref. 8	(p,γ_0) Ref. 9	(d,γ_0) Ref. 18	(d,γ_0) Refs. 19	(γ,d_0) Ref. 17	(t,γ_0) Ref. 15	(e,t_0) Ref. 16	(α,γ_0) Ref. 13	(α,γ_0) Ref. 14	(e,e') Ref. 20
11.1																	
~11.8		~11.6	(11.6)														
~14.1				13.6			13.4										
			~ 15	~15.2	~14.5	14.8	14.7	14.8									14.6
						(15.6)	15.5	15.5									
16.3							16.4						(16.3)		16.4	16.4	
						16.7	16.7	16.7					16.7		16.8		
17.2	~17.2			17.0						(17.2)							~17
										17.7	17.7		(17.5)		17.6		
18.4			~18.5	(~18.5)	~18.5	18.4		18.3									
(19.5)	~18.9			19.5	(~19.5)	19.5	19.5	19.5	19.5						19	19	
20.4			~20.5	20.4	~20.5	20.7	20.5	20.5	20.5					(~20.5)			20.3
22.0				~21.8	(~21.5)		21.7	21.6	21.8		22	22				~21.5	~22
(22.5)	(~22.5)			22.7		(22.5)	22.5	22.4									
23.0			~23		(~23.2)	23.3	23.0	23.0	23.1								
23.8				24.5							24	24					
25.1					(~25)												~25.5
(26.2)					(~26)	25.9	25.8		25.8								
28.2																	
(33)																	
(~36)							~37										

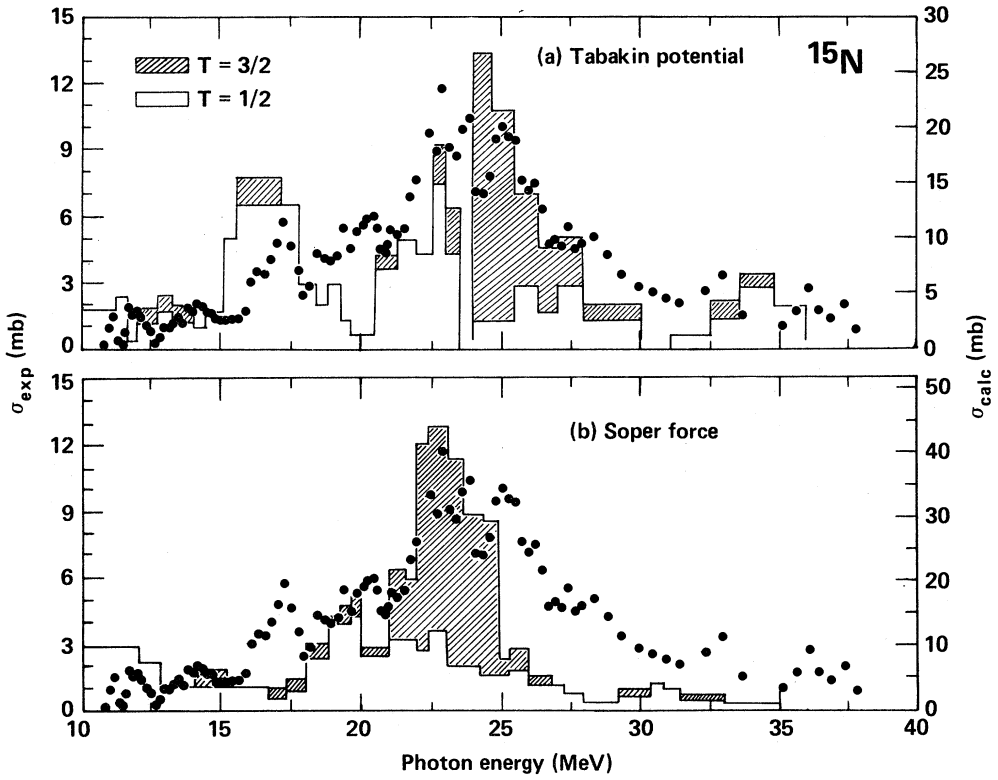

FIG. 5. The $^{15}N(\gamma,n_{tot})$ cross section is compared with the shell-model calculations of Albert *et al.*[28] employing (a) a Tabakin interaction and (b) a δ-function interaction with a Soper mixture of exchange forces. In both cases, the calculated result is the total photonuclear cross section (right-hand scale). The cross-section scales have been chosen to provide a simple visual comparison of the theoretical result with the measured data for the photoneutron channel. One sees that the Tabakin interaction results in a much better fit, in contrast with the cases of ^{13}C and ^{17}O.

cross sections.[29] The histogram shown in Fig. 5(a) represents the results of the calculation of the total photonuclear cross section using the Tabakin interaction where the individual levels have arbitrarily been assigned a width of 2 MeV. This calculation is in substantially better agreement with the present (photoneutron) data than is the (total) cross-section prediction incorporating a δ-function potential with a Soper mixture of exchange forces shown in Fig. 5(b). This Tabakin calculation reproduces the location and width of the GDR satisfactorily. Moreover, when the total photoproton cross section of Denisov *et al.*[5] is added to the present (γ,n_{tot}) results to approximate a photon absorption cross section, the Tabakin interaction becomes an even better description of the cross section than does the Soper mixture. (It should be noted here that comparison of the data with another recent theoretical calculation[34] is not as satisfactory.)

This result is in marked contrast with the cases of ^{13}C and ^{17}O, where the previously reported photoneutron cross sections[21,22] were much better described by the calculation of Albert *et al.*[29] using the Soper mixture. It would appear that this theoretical approach results in a good description of a one-particle two-hole GDR when the Tabakin potential is used *but* gives a better description of the measured cross section for a two-particle one-hole GDR when the Soper mixture is used. We cannot think of any underlying physical reason for this odd result.

In the present case, the assignment of some $T=\frac{1}{2}$ strength near 34 MeV (using the Tabakin interaction) seems to be borne out by the ring-ratio data in the photoneutron channel (Fig. 2). Near 34 MeV a significant increase in the average energy of the emitted photoneutrons suggests that a larger fraction of transitions to low-lying states in ^{14}N is occurring. Because most of the levels of the likely low-energy candidates for population following a predominantly $E1$ excitation mechanism are $T=0$ states in ^{14}N and because the isospin selection rule prohibits decays from $T=\frac{3}{2}$ states in ^{15}N to these levels, it is reasonable to assume that at an excita-

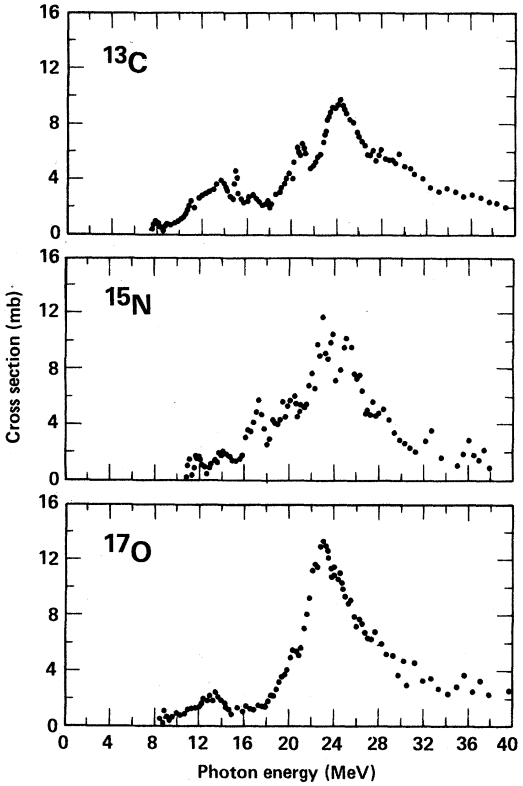

FIG. 6. Comparison is made of the total photoneutron cross sections for (a) ^{13}C, (b) ^{15}N, and (c) ^{17}O, showing the strong similarities among these three cross sections.

tion energy near 34 MeV there is a significant amount of $T=\frac{1}{2}$ strength in the photoabsorption cross section (in qualitative agreement with the calculation of Albert *et al.*[28]). This appears to be a case of isospin splitting in which the $T_<$ strength is fragmented and some of it is pushed up in energy above the GDR. This effect also was seen in ^{13}C (Ref. 21), but in that case the $T_<$ strength at high energy was better predicted by the calculation using the Soper mixture of exchange forces and a δ-function potential.

The failure of these theoretical calculations to account simultaneously for the experimental results for all three odd-A nuclei illustrates the deficiencies of this simplified treatment of the shell-model states and residual interactions, and points out the need for a more sophisticated, general, and self-consistent theoretical approach to the problem. Such an approach would involve more realistic forces, would fit nuclear radii, and would treat a wide range of nuclei.

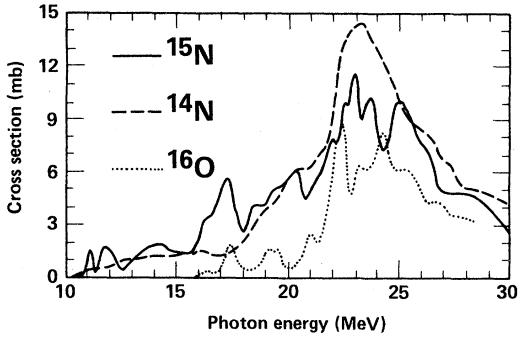

FIG. 7. Comparison is made over the excitation-energy region below 30 MeV of the total photoneutron cross sections for ^{15}N (present work) (solid line), ^{14}N (Ref. 30) (dashed line), and ^{16}O (Refs. 31) (dotted line). All cross sections have been plotted on the same scale. One sees that the GDR for ^{16}O is much narrower than for the others, while that for ^{14}N is the smoothest.

C. Comparison with neighboring nuclei

Figure 6 presents a comparison of the (γ,n_{tot}) cross sections for ^{13}C, ^{15}N, and ^{17}O. An overall similarity of these three cross sections can be seen. Perhaps this is not surprising, since all three nuclei are non-self-conjugate, have nonzero spin, and are one nucleon removed from a $4N$ core nucleus. The energy of the peak of the GDR decreases from about 24 to 23.5 to 23 MeV and the peak photoneutron cross section increases from about 9 to 11 to 13 mb as one goes from ^{13}C to ^{15}N to ^{17}O, in keeping with typical GDR systematics.[1]

On the other hand, Fig. 7 presents a comparison of the (γ,n_{tot}) cross sections up to 30 MeV for ^{14}N, ^{15}N, and ^{16}O. There undoubtedly is a resemblance between the ^{15}N and ^{16}O cross sections. However, significant differences in these cross sections also are apparent; the removal of a proton or of a neutron and a proton from the ^{16}O core has a profound effect upon the photoneutron cross section. Although all three of these cross sections are, to first order, centered about 23.5 MeV, the widths (FWHM of the central peak region) of the nitrogen giant resonances are larger than that for ^{16}O. This extra breadth might arise because a more complex reaction mechanism is acting in the non-closed-shell nuclei: As discussed above, there is good evidence that for ^{15}N and for ^{14}N as well (Refs. 30 and 35) the GDR decays to many highly excited states in the daughter nucleus. However, the splitting of the GDR into its two isospin components for non-self-conjugate nuclei undoubtedly is the primary cause for this broadening. In addition, $E1$ excitation

TABLE IV. Integrated photonuclear cross sections up to 30 MeV.

Nucleus	$\int \sigma(\gamma,n_{\text{tot}})dE_\gamma$ (MeV mb)	TRK units	$\int \sigma(\gamma,p)dE_\gamma$ (MeV mb)	TRK units	Sum[m] TRK units
^{12}C	42[a]	0.23	72[h]	0.40	0.63
^{13}C	95[b]	0.49	55[i]	0.28	0.77
^{14}N	99[c]	0.47	15[j]	0.07	0.54
^{15}N	90[d]	0.40	70[k]	0.31	0.71
^{16}O	48[e]	0.20	87[l]	0.36	0.56
^{17}O	95[f]	0.37	not available		
^{18}O	142[g]	0.53	31[g]	0.12	0.65

[a]Reference 37 plus a small correction for $\sigma(\gamma,n\alpha)$; Ref. 38 gives 37, Ref. 39 gives 46, and Ref. 40 gives 44.
[b]Reference 21.
[c]Reference 30, extrapolated from 29.5 MeV.
[d]Present work.
[e]References 31, extrapolated from 28.0 MeV; Ref. 22 gives 46, Ref. 39 gives 47, and Ref. 41 gives 59.
[f]Reference 22.
[g]Reference 23.
[h]Reference 40 (evaluation of literature).
[i]Reference 42.
[j]Reference 43, extrapolated from 25 MeV, with the aid of Ref. 44 (from Ref. 40).
[k]Reference 5.
[l]References 23 (evaluation of literature); Ref. 40 gives 91.
[m]Note that certain small contributions, such as from the (γ,α), (γ,t), and (γ,γ) channels, are not included.

from the $J=\frac{1}{2}$ and $J=1$ ground states of ^{15}N and ^{14}N can form, respectively, two and three times as many intermediate spin states as transitions from the $J=0$ ^{16}O ground state. The nearly complete lack of intermediate structure for ^{14}N therefore might be accounted for as a smoothing effect owing to the large number of overlapping states. Indeed, this effect has been observed previously for the oxygen-16, -17, and -18 isotopes (Ref. 22) and, even more dramatically, for the magnesium isotopes (Refs. 36) where the photoneutron cross section for ^{25}Mg (spin $\frac{5}{2}$) displays much less clearly delineated structure than those for ^{24}Mg or ^{26}Mg.

The magnitudes of the photoneutron cross sections in Fig. 7 appear to violate the general NZ/A dependence of the TRK sum rule. However, we expect that the magnitude of the photoproton cross sections largely compensates for this behavior. The integrated photoneutron and photoproton cross sections up to 30 MeV are given in Table IV for comparison. For ^{16}O, the integrated photoproton cross section is nearly twice the size of the integrated photoneutron cross section. For ^{14}N it is well established[30,43] that most of the GDR decay proceeds via the (γ,pn) reaction, which results in the emission of a neutron and hence is counted in $\sigma(\gamma,n_{\text{tot}})$. The photoneutron result for ^{15}N is seen to be intermediate between these two examples, as might be expected. Moreover, there is a reasonably good correlation between the ^{15}N and ^{16}O cross sections near 17.3 MeV, where the peak seen in both might reflect the same underlying single-particle amplitudes.

Table IV also contains (γ,n) and (γ,p) data for the other isotopes of carbon and oxygen. It is interesting to note that the sums of these integrated cross sections up to 30 MeV (last column of Table IV) for the self-conjugate nuclei are systematically smaller than those for their non-self-conjugate neighbors. These differences would be even greater if one chose an energy limit below 30 MeV or if one chose to examine σ_{-1} or σ_{-2} rather than σ_{int}, since the (γ,n) and (γ,p) cross sections for these non-self-conjugate nuclei are large at low energies (below $\sim$17 MeV). This is not entirely because the (γ,n) and (γ,p) thresholds are higher for ^{12}C and ^{16}O: The (γ,α) thresholds are low for these nuclei but their (γ,α) cross sections are very small.[40] [In any case the (γ,n) and (γ,p) thresholds for ^{14}N are *lower* than those for ^{15}N.] Rather, it is most likely a manifestation of the presence of a $T_<$ component of the GDR for the non-self-conjugate nuclei (^{13}C, ^{15}N, ^{18}O, and presumably ^{17}O), the bulk of which

lies at lower energies than the $T_>$ component.

VI. CONCLUSIONS

The previously unmeasured photoneutron cross sections for ^{15}N reported in this paper fill an important gap in our knowledge of the photoreactions in the mass-15 nuclei. The transition from the closed-shell ^{16}O nucleus with its single-particle-like GDR cross section to the open-shell ^{14}N case where much of the decay of the GDR proceeds via very complex states in ^{13}N and ^{13}C has been illustrated by this measurement. The GDR for ^{15}N is broader than that for ^{16}O but perhaps it also reflects the same type of 2p-2h interference effects believed responsible for some of the intermediate structure for ^{16}O.

Evidence based upon the measurement of the average neutron energies confirms the nearly 100% branching to the ground state of ^{14}N up to 15 MeV excitation energy (even though the first $T=1$ excited state could be populated). Similar evidence suggests that at high energies ($\sim$33 MeV) there exists appreciable $T_<$ strength. Direct comparison with the ground-state cross section indicates that most of the strength of the GDR proper decays to excited states in ^{14}N.

The data obtained here for a nucleus with 1p-2h GDR configurations are better represented by a shell-model calculation using a Tabakin potential than by one using a Soper mixture of exchange forces. Since this behavior is *opposite* to that for nuclei with 2p-1h GDR configurations (^{13}C and ^{17}O), where the Soper-type calculation was far superior, either a reconsideration of the assumptions and mechanics of this type of shell-model calculation is required or the calculations must be carried out using a more realistic residual interaction in order that a single theoretical treatment be able to describe the photoabsorption mechanism for all of these light nuclei.

Finally, comparison of the present results for ^{15}N with those for neighboring nuclei leads to several observations: (a) that the (γ,n) cross sections for ^{13}C, ^{15}N, and ^{17}O are very similar; (b) that those for ^{14}N, ^{15}N, and ^{16}O are notably different in overall breadth and detailed structure; and (c) that the integrated cross sections for ^{13}C, ^{15}N, and ^{18}O are significantly different from those for ^{12}C, ^{14}N, and ^{16}O in their energy dependence. All of these features can be explained, at least qualitatively, in terms of the spin and isospin properties of the GDR.

ACKNOWLEDGMENTS

This work was carried out at the Lawrence Livermore National Laboratory under the auspices of the U.S. Department of Energy under Contract No. W-7405-ENG-48 and also was supported in part by the Natural Sciences and Engineering Research Council of Canada, the University of Melbourne, and the University of Saskatchewan. We would like to thank Dr. D.D. Faul for his advice and assistance during the data-analysis stage of this work. A preliminary report of this work has appeared as Ref. 45.

---

*Permanent address: Department of Physics, Trent University, Peterborough, Ontario K9J 7B8, Canada.

[1]B. L. Berman and S. C. Fultz, Rev. Mod. Phys. 47, 713 (1975); R. Bergère, in *Photonuclear Reactions I* (Springer, Berlin, 1977), p. 1.

[2]F. W. K. Firk, Annu. Rev. Nucl. Sci. 20, 39 (1970); *Photonuclear Reactions,* edited by E. G. Fuller and E. Hayward (Dowden, Hutchinson, and Ross, Stroudsburg, 1976), parts II and III.

[3]J. L. Rhodes and W. E. Stephens, Phys. Rev. 110, 1415 (1958).

[4]R. Kosiek, Z. Phys. 179, 544 (1964).

[5]V. P. Denisov, L. A. Kulchitskii, and I. Ya. Chubukov, Yad. Fiz. 14, 889 (1971) [Sov. J. Nucl. Phys. 14, 497 (1972)].

[6]G. A. Bartholomew, F. Brown, H. E. Gove, A. E. Litherland, and E. B. Paul, Can. J. Phys. 33, 441 (1955).

[7]M. H. Harakeh, P. Paul, H. M. Kuan, and E. K. Warburton, Phys. Rev. C 12, 1410 (1975).

[8]H. R. Weller, R. A. Blue, N. R. Roberson, D. G. Rickel, S. Maripuu, C. P. Cameron, R. D. Ledford, and D R. Tilley, Phys. Rev. C 13, 922 (1976).

[9]K. A. Snover, J. E. Bussoletti, K. Ebisawa, T. A. Trainor, and A. B. McDonald, Phys. Rev. Lett. 37, 273 (1976).

[10]J. J. Murphy II, Y. M. Shin, and D. M. Skopik, Nucl. Phys. A246, 221 (1975).

[11]J. D. Watson, B. Roth, P. Kuo, J. W. Jury, K. G. McNeill, N. K. Sherman, and W. F. Davidson, Bull. Am. Phys. Soc. 26, 1128 (1981).

[12]S. A. Wender, H. R. Weller, N. R. Roberson, D. R. Tilley, and R. G. Seyler, Phys. Rev. C 25, 89 (1982).

[13]A. Degré, M. Schaeffer, G. Bonneaud, and I. Linck, Nucl. Phys. A306, 77 (1978).

[14]W. Del Bianco, S. Kundo, and J. Kim, Can. J. Phys. 55, 302 (1977).

[15]M. Schaeffer, A. Degré, M. Suffert, G. Bonneaud, and I. Linck, Nucl. Phys. A275, 1 (1977).
[16]J. Uegaki, J. Asai, M. K. Leung, J. J. Murphy II, Y. M. Shin, and D. M. Skopik, Can. J. Phys. 57, 1059 (1979).
[17]D. M. Skopik, J. J. Murphy II, H. R. Weller, R. A. Blue, N. R. Roberson, S. A. Wender, and D. R. Tilley, Phys. Rev. C 20, 409 (1979).
[18]H. R. Weller and R. A. Blue, Nucl. Phys. A211, 221 (1973).
[19]W. Del Bianco, S. Kundu, and J. Kim, Nucl. Phys. A270, 45 (1976); W. Del Bianco, N. Marquardt, K. Farzine, and H. V. Buttlar, Can. J. Phys. 56, 3 (1978).
[20]E. J. Ansaldo, J. C. Bergstrom, and R. Yen, Phys. Rev. C 18, 597 (1978).
[21]J. W. Jury, B. L. Berman, D. D. Faul, P. Meyer, K. G. McNeill, and J. G. Woodworth, Phys. Rev. C 19, 1684 (1979).
[22]J. W. Jury, B. L. Berman, D. D. Faul, P. Meyer, and J. G. Woodworth, Phys. Rev. C 21, 503 (1980).
[23]J. G. Woodworth, K. G. McNeill, J. W. Jury, R. A. Alvarez, B. L. Berman, D. D. Faul, and P. Meyer, Phys. Rev. C 19, 1667 (1979); B. L. Berman, D. D. Faul, R. A. Alvarez, and P. Meyer, Phys. Rev. Lett. 36, 1441 (1976).
[24]B. L. Berman, D. D. Faul, P. Meyer, and D. L. Olson, Phys. Rev. C 22, 2273 (1980).
[25]D. D. Faul, B. L. Berman, P. Meyer, and D. L. Olson, Phys. Rev. C 24, 849 (1981).
[26]R. F. Fraser, R. K. Garnsworthy, and B. M. Spicer, Nucl. Phys. A156, 489 (1970).
[27]R. F. Barrett, R. F. Fraser, and P. P. Delsanto, Phys. Lett. 40B, 326 (1972).
[28]D. J. Albert, A. Nagl, J. George, R. F. Wagner, and H. Uberall, Phys. Rev. C 16, 503 (1977).
[29]D. J. Albert, J. George, and H. Uberall, Phys. Rev. C 16, 2452 (1977).
[30]B. L. Berman, S. C. Fultz, J. T. Caldwell, M. A. Kelly, and S. S. Dietrich, Phys. Rev. C 2, 2318 (1970).
[31]R. L. Bramblett, J. T. Caldwell, R. R. Harvey, and S. C. Fultz, Phys. Rev. 133, B869 (1964); J. T. Caldwell, R. L. Bramblett B. L. Berman, R. R. Harvey, and S. C. Fultz, Phys. Rev. Lett. 15, 976 (1965).
[32]B. H. Patrick, E. M. Bowey, and E. G. Muirhead, J. Phys. G 10, 751 (1976).
[33]W. J. O'Connell and S. S. Hanna, Phys. Rev. C 17, 892 (1978).
[34]H. R. Kissener and R. A. Eramzhyan (unpublished), reproduced in B. S. Ishkhanov, I. M. Kapitonov, V. G. Neudachin, and R. A. Eramzhyan, Phys. Elem. Part. Atom. Nucl. 12, 905 (1981); and H. R. Kissener, private communication.
[35]J. W. Jury, C. K. Ross, and N. K. Sherman, Nucl. Phys. A337, 503 (1980).
[36]R. A. Alvarez, B. L. Berman, D. R. Lasher, T. W. Phillips, and S. C. Fultz, Phys. Rev. C 4, 1673 (1971); S. C. Fultz, R. A. Alvarez, B. L. Berman, M. A. Kelly, D. R. Lasher, T. W. Phillips, and J. McElhinney, *ibid.* 4, 149 (1971).
[37]F. J. Kline and E. Hayward, Phys. Rev. C 17, 1531 (1978).
[38]S. C. Fultz, J. T. Caldwell, B. L. Berman, R. L. Bramblett, and R. R. Harvey, Phys. Rev. 143, 790 (1966).
[39]U. Kneissl, E. A. Koop, G. Kuhl, K. H. Leister, and A. Weller, Nucl. Instrum. Methods 127, 1 (1975).
[40]E. G. Fuller, private communication.
[41]A. Veyssière, H. Beil, R. Bergère, P. Carlos, A. Leprêtre, and A. de Miniac, Nucl. Phys. A227, 513 (1974).
[42]B. C. Cook, Phys. Rev. 106, 300 (1957).
[43]J. E. E. Baglin, E. J. Bentz, and R. W. Carr, Phys. Rev. C 10, 24 (1974).
[44]P. Paul, H. S. Kuan, and E. K. Warburton, Nucl. Phys. A254, 1 (1975).
[45]J. W. Jury, B. L. Berman, J. G. Woodworth, K. G. McNeill, M. N. Thompson, and R. E. Pywell, Bull. Am. Phys. Soc. 26, 1128 (1981).